Evidence for *Elizabethkingia anophelis* Transmission from Mother to Infant, Hong Kong

Susanna K.P. Lau,[1] Alan K.L. Wu,[1] Jade L.L. Teng,[1] Herman Tse,[1] Shirly O.T. Curreem, Stephen K.W. Tsui, Yi Huang, Jonathan H.K. Chen, Rodney A. Lee, Kwok-Yung Yuen, Patrick C.Y. Woo

Elizabethkingia anophelis, recently discovered from mosquito gut, is an emerging bacterium associated with neonatal meningitis and nosocomial outbreaks. However, its transmission route remains unknown. We use rapid genome sequencing to investigate 3 cases of *E. anophelis* sepsis involving 2 neonates who had meningitis and 1 neonate's mother who had chorioamnionitis. Comparative genomics revealed evidence for perinatal vertical transmission from a mother to her neonate; the 2 isolates from these patients, HKU37 and HKU38, shared essentially identical genome sequences. In contrast, the strain from another neonate (HKU36) was genetically divergent, showing only 78.6% genome sequence identity to HKU37 and HKU38, thus excluding a clonal outbreak. Comparison to genomes from mosquito strains revealed potential metabolic adaptations in *E. anophelis* under different environments. Maternal infection, not mosquitoes, is most likely the source of neonatal *E. anophelis* infections. Our findings highlight the power of genome sequencing in gaining rapid insights on transmission and pathogenesis of emerging pathogens.

Microbial genome sequencing can enhance diagnosis and control of infectious diseases (*1,2*). Its ultimate molecular resolution is superior to other phenotypic and genotypic tests and enables not only rapid microbial identification but also characterization of transmission events. The technique has been applied in large-scale infectious disease outbreaks such as those caused by *Escherichia coli* O104:H4, *Staphylococcus aureus*, *Streptococcus pyogenes*, *Enterococcus faecium*, *Pseudomonas aeruginosa*, *Vibrio cholerae*, and mycobacteria (*3–14*). However, the routine application of this method in diagnostic microbiology and infection control, especially for less well-defined, emerging pathogens, is yet to be explored.

Elizabethkingia anophelis is a recently discovered bacterium isolated from the midgut of the *Anopheles gambiae* mosquito in 2011 (*15*). The genus *Elizabethkingia* also includes *E. meningoseptica* (previously named *Chryseobacterium/Flavobacterium meningosepticum*) and *E. miricola* (*16*). *E. meningoseptica* causes neonatal sepsis and infections in immunocompromised persons. *E. anophelis* has also recently been reported to cause neonatal meningitis in the Central African Republic, and a nosocomial outbreak was reported in an intensive care unit in Singapore (*17–19*). However, the role of mosquitoes or other sources in the transmission of *E. anophelis* remains unclear.

In 2012, we encountered 3 cases of *Elizabethkingia* sepsis associated with meningitis in 2 neonates and chorioamnionitis in a neonate's mother in a hospital in Hong Kong. Three strains of *Elizabethkingia*-like, gram-negative bacilli sharing similar phenotypic characteristics were isolated from the 3 patients, but confident identification results were not obtained by matrix-assisted laser desorption ionization/time-of-flight (MALDI-TOF) mass spectrometry and 16S rRNA gene sequencing. Moreover, clinical and microbiological data did not provide adequate clues about the possible transmission route. We therefore attempted to use draft genome sequencing to rapidly dissect transmission pathways and confirm the identity of the species.

Materials and Methods

Setting and Patients

The 3 patients were hospitalized in an acute regional hospital, Pamela Youde Nethersole Eastern Hospital, which is situated in the eastern area of Hong Kong Island. This study was approved by the Institute Review Board, Hospital Authority, Hong Kong (reference HKEC-2013-051).

Author affiliations: The University of Hong Kong, Hong Kong (S.K.P. Lau, J.L.L. Teng, H. Tse, S.O.T. Curreem, Y. Huang, J.H.K. Chen, K.-Y. Yuen, P.C.Y. Woo); State Key Laboratory of Emerging Infectious Diseases, Research Centre of Infection and Immunology, Carol Yu Centre for Infection, Hong Kong (S.K.P. Lau, H. Tse, K.Y. Yuen, P.C.Y. Woo); Pamela Youde Nethersole Eastern Hospital, Hong Kong (A.K.L. Wu, R.A. Lee); School of Biomedical Sciences, The Chinese University of Hong Kong, Hong Kong (S.K.W. Tsui)

DOI: http://dx.doi.org/10.3201/eid2102.140623

[1]These authors contributed equally to this article.

Microbiological Methods

Bacterial cultures and phenotypic identification were performed according to standard protocols by using the Vitek II system (bioMérieux, Marcy l'Etoile, France). Antimicrobial drug susceptibility testing was performed by E-test method for vancomycin and Kirby-Bauer disk diffusion for other drugs; because interpretative criteria for *Elizabethkingia* were lacking, results were interpreted according to Clinical and Laboratory Standards Institute for *Pseudomonas aeruginosa* (*20*). MALDI-TOF mass spectrometry was performed by the direct transfer method as described previously (*21*), with modifications by using the Bruker Daltonics microflex LT system with Reference Library Biotyper version 3.1 (Bruker Daltonik GmbH, Leipzig, Germany). Full 16S rRNA gene amplification and squencing were performed according to previously published protocols with modifications (*22,23*). Pulsed-field gel electrophoresis (PFGE) was performed by using the CHEF Mapper XA system (Bio-Rad, Hercules, CA, USA) and restriction endonuclease *Xba*I as described previously (*8,22*).

Draft Genome Sequencing and Analysis

The draft genome sequences of the 3 *E. anophelis* strains were determined by high-throughput sequencing with the Illumina HiSeq 2500 system (Illumina, San Diego, CA, USA). Samples of 50 ng of genomic DNA were extracted by using a genomic DNA purification kit (QIAGEN, Hilden, Germany) from cultures grown overnight on blood agar at 37°C, as described previously (*24,25*). Each sample was sequenced by 151-bp paired-end reads with mean library size of 350 bp. Sequencing errors were corrected by k-mer frequency spectrum analysis using SOAPec (http://soap.genomics.org.cn/about.html). De novo assembly was performed in SOAPdenovo2 (http://soap.genomics.org.cn/soapdenovo.html). Prediction of protein coding regions and automatic functional annotation was performed by using Glimmer3 (*26*) and the RAST (Rapid Annotations using Subsystem Technology) server (*27*). Antibiotic resistomes were identified by using the Antibiotic Resistance Genes Database (*28*). BLASTn comparisons were run in BLAST+ (http://blast.ncbi.nlm.nih.gov/Blast.cgi) with an E-value cutoff of 10.0. In addition, manual annotation was performed on putative virulence and antibiotic resistance genes by protein domain predictions and multiple sequence alignments with orthologous genes. Intergenomic distance was calculated by using Genome-to-Genome Distance Calculator 2.0 (http://ggdc.dsmz.de/distcalc2.php) (*29*).

Results

Patients

In July 2012, a 21-day-old male neonate (patient 1) was admitted to Pamela Youde Nethersole Eastern Hospital for fever of 1 day's duration. He was born at the same hospital 21 days earlier at 41 weeks' gestation by vaginal delivery and was discharged on day 3. Physical examination did not show obvious infective focus. Serum C-reactive protein (CRP) was elevated to 109 mg/L. Lumbar puncture was performed; analysis of cerebrospinal fluid (CSF) showed polymorph pleocytosis, elevated protein levels, and low glucose levels (Table). Treatment was initiated for bacterial meningitis with empirical intravenous ampicillin and cefotaxime. Blood and CSF cultures recovered a gram-negative bacillus, designated HKU36. Antimicrobial drugs were changed to vancomycin, piperacillin, and rifampin on day 3. The patient was discharged after 3 weeks of intravenous drug treatment, without neurologic sequelae (Figure 1). The neonate's mother was admitted to the same hospital 1 day after the infant's admission for postpartum fever, chills, rigor, and abdominal pain. Transvaginal ultrasound showed no retained gestational products. Serum CRP level was elevated to 109 mg/L; however, blood cultures were negative. She was treated with intravenous cefuroxime and metronidazole and discharged on day 6 with oral cefuroxime and metronidazole.

In November 2012, a 33-year-old woman in week 30 of pregnancy (patient 2) was admitted to the same hospital because of prolonged premature rupture of membranes. She stayed at the same antenatal ward and in the same cubicle as the mother of patient 1 (Figure 1). Fever developed in the patient 3 days after admission, and clinical tests showed peripheral leukocytosis with neutrophilia (Table). Serum CRP was elevated to 108 mg/L. Treatment with intravenous penicillin G was commenced, and an emergency lower segment cesarean section was performed. Placental and uterine swab cultures recovered a gram-negative bacillus, designated HKU37. Blood cultures were negative. Antimicrobial drug treatment was changed to cefuroxime and metronidazole, followed by oral ciprofloxacin for 1 week. Her fever subsided, and she was discharged on day 8.

The baby girl (patient 3) of patient 2 was pale and flaccid at birth; apnea of prematurity developed, requiring cardiopulmonary resuscitation. Peripheral leukopenia and metabolic acidosis were also detected, and serum CRP level was elevated to 70.6 mg/L. Chest radiograph showed bilateral ground-glass appearance. Lumbar puncture was performed, and CSF showed lymphocytic pleocytosis with elevated protein levels and low glucose levels (Table). Ultrasound of the brain showed grade I to II intraventricular hemorrhages. Empirical intravenous ampicillin and cefotaxime at meningitic dose was started. Blood and CSF cultures recovered a gram-negative bacillus, designated HKU38. Antimicrobial drug therapy was changed to intravenous vancomycin, piperacillin/tazobactam, and rifampin on day 3, continuing for 3 weeks. Necrotizing enterocolitis and neonatal jaundice developed, but both resolved with

Table. Clinical characteristics and results of testing for 3 patients infected with *Elizabethkingia anophelis*, Hong Kong, 2012*

Characteristics	Patient 1	Patient 2†	Patient 3
Patient age/sex	21 d/M	33 y/F	0 d/F
Signs/symptoms	Fever	Fever, PPROM	Apnea at birth
Blood test results			
Total leukocytes, × 10^9 cells/L	16.0 (5.0–19.5)	15.2 (3.7–9.3)	5.1 (10.0–27.0)
Neutrophils, × 10^9 cells/L	6.8 (2.0–9.5)	12.5 (1.8–6.2)	1.2 (5.0–17.0)
Lymphocytes, × 10^9 cells/L	6.8 (2.5–11.0)	1.7 (1.0–3.2)	3.4 (3.0–10.0)
Monocytes, × 10^9 cells/L	2.3 (0.2–1.2)	0.8 (0.2–0.7)	0 (0.5–2.0)
Hemoglobin, g/dL	14.0 (11.0–19.0)	10.7 (11.5–15.4)	16.1 (13.5–19.5)
Platelets, × 10^9/L	180 (180–460)	241 (160–420)	186 (100–300)
C-reactive protein, mg/L	109 (<8.0)	108 (<5.0)	70.6 (<8.0)
CSF test results			
Total leukocytes, × 10^6 cells/L	1,445	NA	5,850
Polymorphs, %	67	NA	1
Lymphocytes, %	33	NA	99
Protein, g/L	1.33 (0.15–0.45)	NA	2.69 (0.15–0.45)
Glucose, mmol/L	2.2 (2.8–4.4)	NA	1.5 (2.8–4.4)
CSF/serum glucose, %	38	NA	24
Positive culture sites for *E. anophelis*	Blood, CSF	Placental swab, uterine swab	Blood, CSF
Phenotypic characteristics of isolates			
Colony pigment	Pale yellow	None	None
Citrate utilization	Negative	Delayed positive	Delayed positive
Antimicrobial drug susceptibilities of isolates			
Ampicillin	Resistant	Resistant	Resistant
Pipercillin	Susceptible	Susceptible	Susceptible
Cefoperazone/sulbactam	Susceptible	Susceptible	Susceptible
Cefotaxime	Intermediate	Resistant	Resistant
Ceftazidime	Resistant	Resistant	Resistant
Imipenem	Resistant	Resistant	Resistant
Amikacin	Resistant	Resistant	Resistant
Gentamicin	Resistant	Resistant	Resistant
Kanamycin	Resistant	Resistant	Resistant
Streptomycin	Resistant	Resistant	Resistant
Tobramycin	Resistant	Resistant	Resistant
Ciprofloxacin	Susceptible	Susceptible	Susceptible
Moxifloxacin	Susceptible	Susceptible	Susceptible
Tetracycline	Resistant	Resistant	Resistant
Trimethoprim/sulfamethoxazole	Susceptible	Susceptible	Susceptible
Rifampin	Susceptible	Susceptible	Susceptible
Chloramphenicol	Resistant	Resistant	Resistant
Vancomycin MIC, µg/mL	16	4	4
Antimicrobial drug regimen	Ampicillin + cefotaxime; vancomycin + piperacillin + rifampin	Penicillin G; cefuroxime + metronidazole; ciprofloxacin	Ampicillin + cefotaxime; vancomycin + pipercillin/tazobactam + rifampin
Complications	None	None	Respiratory distress, intraventricular hemorrhage

*Reference ranges are shown in parentheses. PPROM, prolonged premature rupture of membranes; CSF, cerebrospinal fluid.
†Mother of patient 3.

treatment (Figure 1). The infant was discharged on day 54 without neurologic sequelae.

Clinical and Microbiological Investigations

The 3 isolates from these patients, HKU36–38, were nonmotile, oxidase-positive, non–glucose-fermenting, gram-negative bacilli. Their phenotypic characteristics are summarized in the Table and online Technical Appendix Table 1 (http://wwwnc.cdc.gov/EID/article/21/2/14-0623-Techapp1.pdf). The isolates were identified as *E. meningoseptica* by using the Vitek II identification system (bioMérieux, Marcy L'Étoile, France). However, MALDI-TOF mass spectrometry identified strains HKU37 and HKU 38 as *E. meningoseptica* (best match to *E. meningoseptica* strain 002_NEB14 NFI, with scores of 2.106 and 2.007, respectively), whereas strain HKU36 was only identified to the genus level as *Elizabethkingia* species (best match to *E. meningoseptica* strain 002_NEB14 NFI, with score of 1.853) (online Technical Appendix Figure 1). The isolates' 16S rRNA gene sequences exhibited 99.1%–99.9% nucleotide identities to those of *E. anophelis* type strain R26^T (GenBank accession no. EF426425) and 97.4%–99.9% nucleotide identities to those of *E. meningoseptica* strains deposited in GenBank (GenBank accession nos. HM056770.1, GU180602.1, JQ673498.1, FJ816020, AVCQ01000012, FJ839441.1, JN201943.1, and AJ704540).

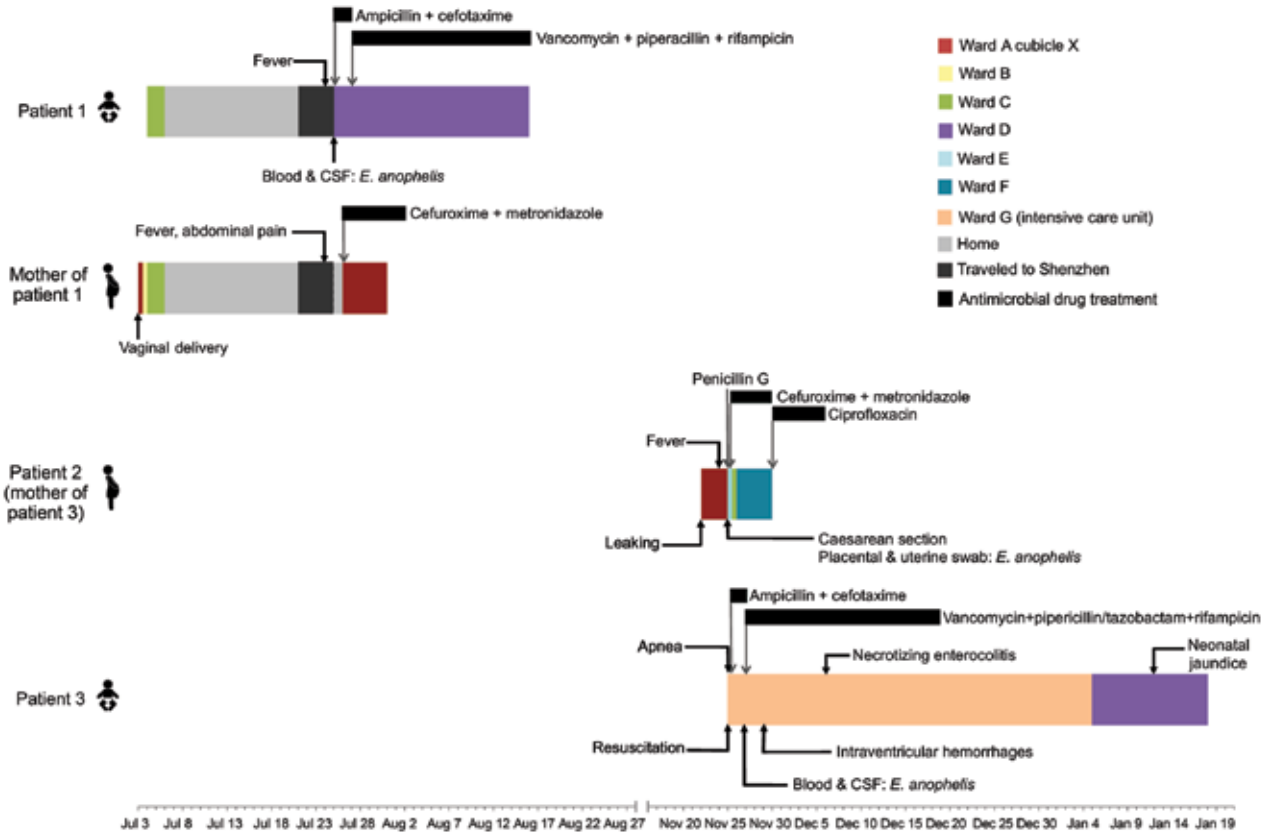

Figure 1. Clinical course of illness in 3 patients infected with *Elizabethkingia anophelis* in whom sepsis developed and the mother of patient 1, who had culture-negative postpartum fever, Hong Kong, 2012. Locations where patients were treated at the hospital and times when they were home are noted. CSF, cerebrospinal fluid; leaking, leaking of amniotic fluid (membrane rupture).

The high sequence identities to both *E. anophelis* and *E. meningoseptica* made the species identity of the 3 strains uncertain, despite 16S rRNA gene sequencing. Moreover, the strains exhibited minor differences in phenotypes and antibiogram (Table). Further, because the mothers stayed in the same ward before delivery (although 4 months apart), concerns of a possible nosocomial outbreak were raised. However, environmental and water samples from the hospital and patients' homes were culture-negative for *E. anophelis*. A program of enhanced infection control measures was enforced in the hospital, and no further cases were identified.

Genome Sequencing and Comparative Analysis of *E. anophelis* Genomes

We sequenced the draft genomes of strains HKU36–38 to investigate their genetic relatedness and confirm their species identity. Sequencing generated 11–15 million paired-end reads per strain (estimated 410–540-fold coverage). After de novo assembly, the 3 draft genomes ranged from 3.92–3.99 Mb in length (G + C content 35.4%–35.8%) and were distributed in 42–52 large (>500 bp) contigs (EMBLaccessionnos.CBYD010000001–CBYD010000042, CBYE010000001–CBYE010000032, CBYF010000001–CBYF010000038; online Technical Appendix Table 2). These contigs contained 3,654–3,667 predicted protein-coding genes (Figure 2, panel A). Using Genome-to-Genome Distance Calculator for intergenomic distance estimation, which enabled genome-based species delineation analogous to traditional DNA–DNA hybridization method, we found that these genomes shared 78.3%–85.4% nucleotide identities to the draft genome sequence of *E. anophelis* type strain R26^T, the initial isolate from an *Anopheles gambiae* mosquito (GenBank accession no. NZ_ANIW00000000.1). However, the genomes shared only 23.6%–23.7% nucleotide identities to the draft genome sequence of *E. meningoseptica* type strain ATCC 13253^T (GenBank accession no. BARD00000000.1) (Figure 2, panel B). Phylogenetic analysis using the draft genomes and concatenated sequences of 69 housekeeping genes also supported the identification of the 3 strains as *E. anophelis* (Figure 3; online Technical Appendix Figure 2).

The sequences from 52 contigs of strain HKU37 demonstrated 99.4% nucleotide identity to those from 46 contigs of strain HKU38, indicating that these draft genomes

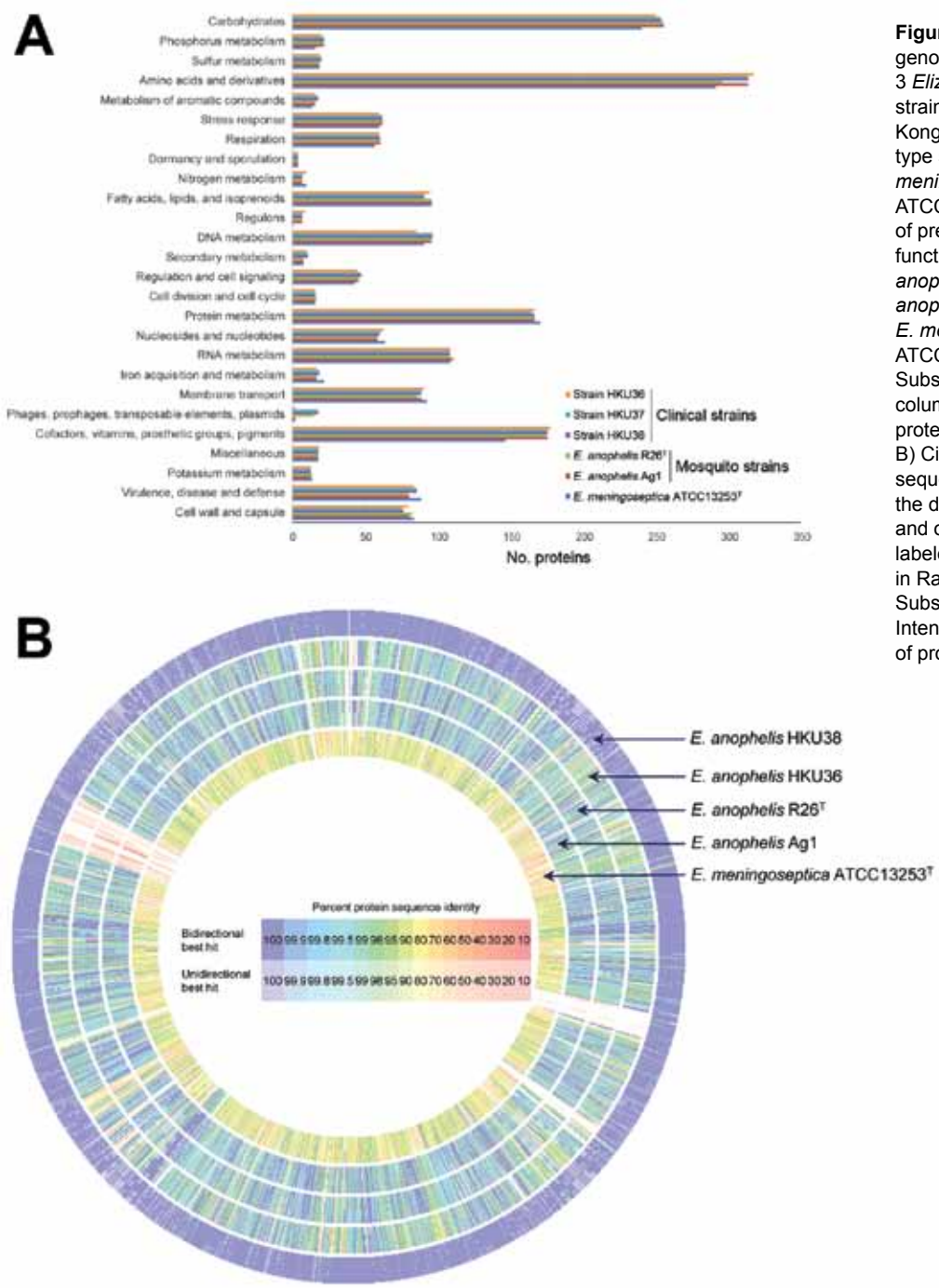

Figure 2. Comparison of draft genome sequence data of the 3 *Elizabethkingia anophelis* strains from patients in Hong Kong (HKU36–38), *E anophelis* type strain R26T, and *E. meningoseptica* type strain ATCC 13253T. A) Distributions of predicted coding sequence function in genomes of *E. anophelis* strains HKU36–38, *E. anophelis* type strain R26T, and *E. meningoseptica* type strain ATCC 13253T according to SEED Subsystems are shown. The columns indicate the number of proteins in different subsystems. B) Circular representation of sequence comparison between the draft genome of strain HKU37 and other draft genomes as labeled. Comparison generated in Rapid Annotations using Subsystem Technology (27). Intensity of color indicates degree of protein identity.

are essentially identical (Figure 2, panel B, and Figure 3). The small intergenomic distance can be explained by slight differences in coverage or contig assembly; sequences of 2,000 high-coverage protein-coding genes were identical between HKU37 and HKU38. In contrast, these sequences demonstrated only 78.6% nucleotide identity to those from the 42 contigs of strain HKU36, indicating that strain HKU36 is genetically divergent (Figure 2, panel B, and Figure 3), consistent with PFGE patterns (Figure 4). Moreover, a potential genetic island consisting of conjugative transposable elements was found in strains HKU37 and HKU38 but not in HKU36. Our results exclude a clonal outbreak, but the extremely close genetic relatedness between strains HKU37 and HKU38 provides evidence for vertical transmission from patient 2 to patient 3 (mother to infant).

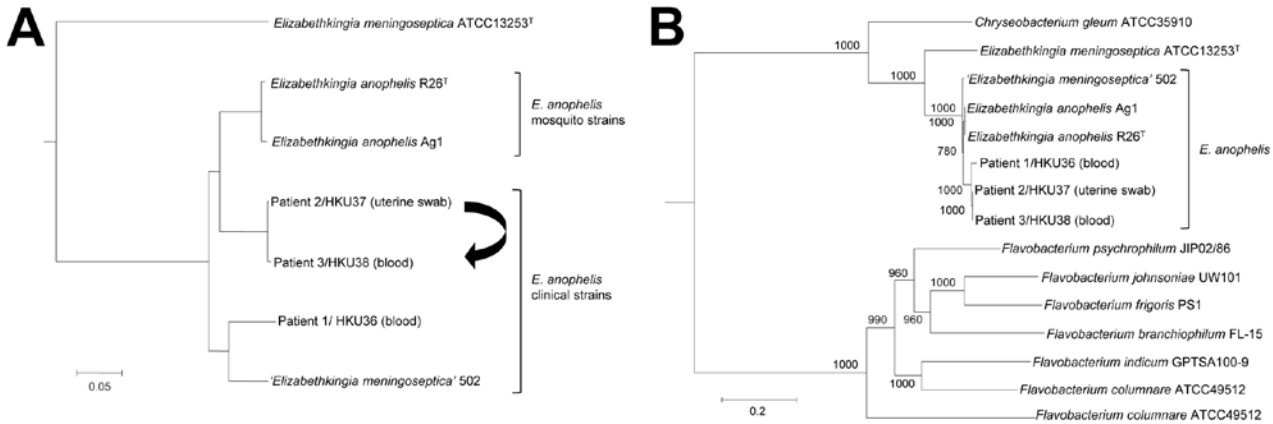

Figure 3. Phylogenetic trees constructed by using draft genome sequences and concatenated sequences of 69 housekeeping genes of 3 *Elizabethkingia anophelis* strains from patients in Hong Kong (HKU36–38). A) Neighbor-joining tree constructed on the basis of draft genome sequences using by using Genome-to-Genome Distance Calculator 2.0 (http://ggdc.dsmz.de/distcalc2.php; formula 1) and *Chryseobacterium gleum* ATCC 35910 as the root. Arrow indicates route of mother-to-neonate transmission. B) Maximum-likelihood tree constructed on the basis of 69 housekeeping genes, showing the relationship of *E. anophelis* strains HKU36–38 to related bacterial species, using RAxML version 7.2.8 (http://sco.h-its.org/exelixis/software.html) and *Weeksella virosa* DSM 16922 as the root. A total of 78,520 nt positions were included in the analysis. Bootstrap values were calculated from 1,000 replicates. Scale bars indicate mean number of nucleotide substitutions per site on the respective branches. Gene names and accession numbers are given as cited in GenBank (online Technical Appendix Table 2, http://wwwnc.cdc.gov/EID/article/21/2/14-0623-Techapp1.pdf). '*E. meningoseptica*' strain 502 is a misidentified isolate that actually belongs to *E. anophelis* on the basis of draft genome sequencing.

Potential Virulence Factors and Resistance Genes in *E. anophelis*

The association of *E. anophelis* with neonatal meningitis in this and previous reports (*17,18*) suggests that the bacterium may possess virulence factors that enable it to invade the central nervous system. The 3 draft genomes we identified contain homologs of several virulence genes found in *Listeria monocytogenes*, which also causes neonatal meningitis. These genes include cell wall hydrolase A, which enables host cell invasion; phosphatidylinositol-specific phospholipase (PlcA) and listeriolysin O (LLO), which enable escape from the primary vacuole of macrophages, and genes that enable survival in the secondary vacuole of macrophages; and virulence cluster protein B (VclB). Phosphatidylinositol-specific phospholipase, listeriolysin O, and virulence cluster protein B are located in the *Listeria* pathogenicity island LIPI-1 (*30,31*). Moreover, the 3 genomes we identified contain homologs of arylsulfatase and genes that enable invasion of brain endothelial cells, which contribute to the ability of *Escherichia coli* to cross the blood–brain barrier in neonatal meningitis (*32*).

Vertical transmission of *E. anophelis* from mother to infant also suggests that the bacterium may be able to colonize the vagina before causing ascending chorioamnionitis in the mother and neonatal infection through transplacental spread. A homologof the gene encoding agmatine deiminase, AgDI, which mediates acid tolerance in *L. monocytogenes* (*33*), was found in the *E. anophelis* genomes. Further studies may investigate the possible role of AgDI and potential adherence factors for vaginal colonization in *E. anophelis*.

Similar to *E. meningoseptica*, the 3 *E. anophelis* isolates we identified are resistant to multiple antimicrobial drugs. We found various antimicrobial resistance genes consistent with their resistance phenotypes, including metallo-β-lactamase (bla_{GOB-1} and *blaB14* in strain HKU36 and a novel bla_{GOB} and *blaB1* in strains HKU37 and HKU38) and extended-spectrum β-lactamase ($blaA_{CME-1}$ in strains HKU37 and HKU38 and a potential novel $blaA_{CME-1}$ variant in strain HKU36). A comparison of these β-lactamases to their corresponding orthologs in *E. meningoseptica* genomes revealed only 74%–85% amino acid identities, indicating that *E. anophelis* and related bacteria are potential reservoirs of novel β-lactamase genes (*19,34,35*). Other antimicrobial resistance genes found included multidrug-resistance efflux pumps (ATP binding cassette superfamily, major facilitator superfamily, resistance-nodulation-division families, multidrug and toxic-compound extrusion family) that potentially carry resistance to a variety of compounds; chloramphenicol acetyltransferase; aminoglycoside 6-adenyltransferase; and tetracycline resistant gene. Moreover, a putative *tetX* gene was also identified; this gene encodes a predicted flavin-dependent monooxygenase with tetracycline/tigecycline-degrading activity, although the 3 strains we identified are only resistant to tetracycline but remained susceptible to other related drugs, including tigecycline.

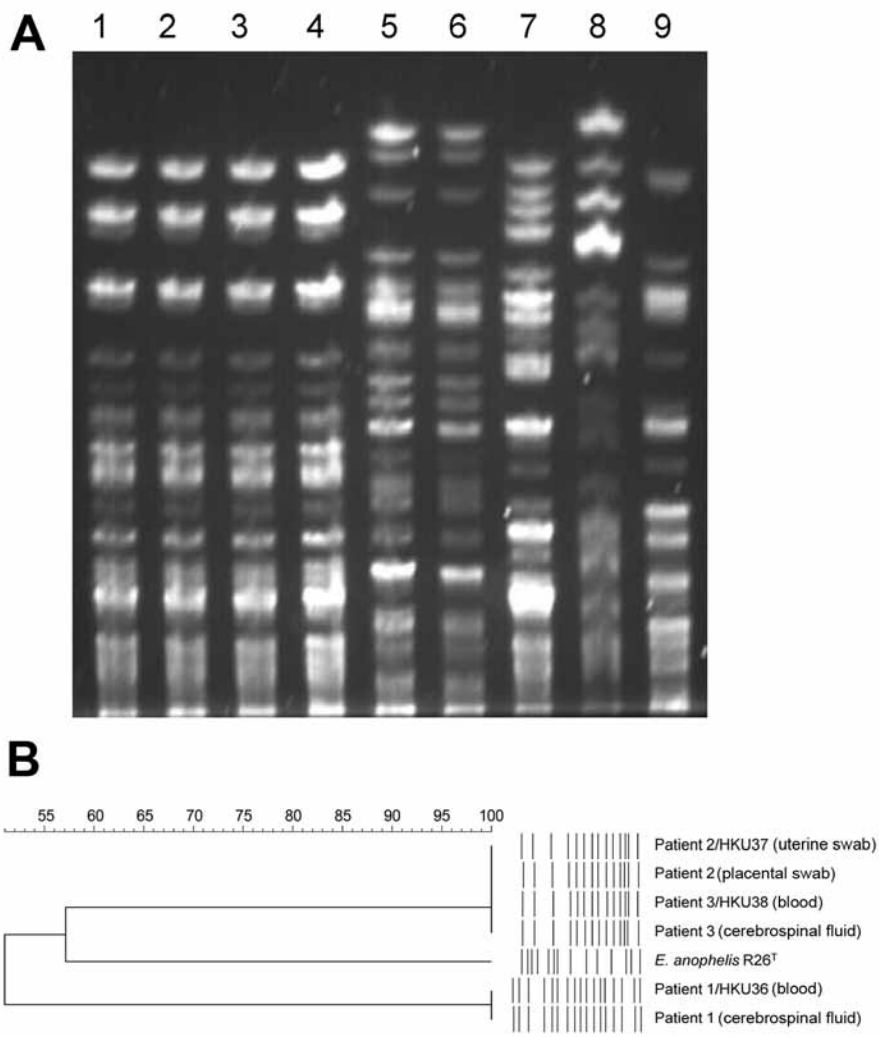

Figure 4. Pulsed-field gel electrophoresis (PFGE) analysis of samples from patients in Hong Kong showing 3 *Elizabethkingia anophelis* strains compared with reference *Elizabethkingia* isolates. A) PFGE performed by using CHEF Mapper XA system (Bio-Rad, Hercules, CA, USA) and restriction endonuclease XbaI shows that isolates from patient 2 and patient 3 are indistinguishable, wheras isolates from patient 1 possess distinct PFGE patterns. Lane 1, *E. anophelis* strain HKU37 from uterine swab specimen of patient 2; lane 2, placental swab specimen from patient 2; lane 3, *E. anophelis* strain HKU38 from blood of patient 3; lane 4, cerebrospinal fluid from patient 3; lane 5, *E. anophelis* strain HKU36 from blood of patient 1; lane 6, cerebrospinal fluid from patient 1; lane 7, *E. anophelis* type strain R26^T; lane 8, *E. meningoseptica* type strain ATCC 13253^T; lane 9, *E. miricola* type strain LMG22470T. B) Dendrogram constructed with PFGE data by similarity and clustering analysis using the Dice coefficient (1% tolerance and 0.5% optimization) and the unweighted pair-group method using average linkages with GelCompar II (Applied Maths, Sint-Martens-Latem, Belgium).

Comparison of Genomes from Human and Mosquito *E. anophelis* Strains

E. anophelis strains R26^T and Ag1 were isolated from mosquitoes (*35*). Compared with those strains, the genomes of the 3 strains we identified possessed 33 unique hypothetical proteins. Moreover, the genetic island consisting of conjugative transposable elements found in strains HKU37 and HKU38 was also absent in the mosquito strains. In contrast to the mosquito strains, which possessed genes encoding for xylose isomerase (XylA) and xylulose kinase (XylB), these 2 genes were absent in the 3 strains we identified. This finding may reflect different requirements for sugar metabolism in *E. anophelis* under different environments. Notably, despite the presence of XylA and XylB, *E. anophelis* mosquito strain R26^T did not produce acid from xylose (*15*). However, this finding does not exclude the strain's ability to metabolize xylose, as D-xylulose 5-phosphate, the product of XylA and XylB, can be used as a substrate for the pentose-phosphate pathway. XylA and XylB were also absent in the genome of *E. meningoseptica* type strain ATCC 13253^T, which suggests that mosquito strains of *E. anophelis* may be evolutionarily distinct from clinical strains of *E. anophelis* and *E. meningoseptica*. More genome sequence data from other clinical and environmental strains of *E. anophelis* may shed light on the ecology, biology, and pathogenesis of *E. anophelis*.

Discussion

This study demonstrates the power of draft genome sequencing to rapidly dissect transmission pathways for emerging bacterial infections. Our results showed that vertical perinatal transmission had occurred from patient 2, a pregnant woman who had chorioamnionitis, to patient 3, a neonate who had early onset neonatal meningitis. The infective source for patients 2 and 3 was unlikely to have been patient 1 or his mother. However, we speculate that the mother of patient 1 might also have had *E. anophelis* chorioamnionitis, as evidenced by postpartum fever and

abdominal pain, which resulted in late-onset meningitis in her son owing to fastidious bacterial growth. Although strain HKU36 did not belong to the same clone as strains HKU37/38, a polyclonal outbreak of *E. anophelis* sepsis in the labor ward, in which case an environmental source is likely, could not be excluded.

The discovery of *E. anophelis* in mosquito gut has raised suspicion that mosquitoes are the source of neonatal meningitis cases in Africa (*17*). Although *Anopheles* mosquitoes are not found in Hong Kong, the role of local mosquitoes as reservoirs for *E. anophelis* remains unknown. Nonetheless, the vertical transmission demonstrated in 1 neonate makes mosquitoes unlikely as vehicles of transmission in our cases.

Our report provides genomic evidence for vertical transmission in neonatal meningitis. Whereas we cannot ascertain how the mother(s) acquired the infection, our results prompt further work to assess the importance of maternal source in neonatal meningitis caused by *E. anophelis* and other bacterial agents. Maternal colonization with Lancefield group B streptococcus (GBS) during pregnancy is the primary risk factor for early onset neonatal disease. However, direct microbiological evidence for vertical transmission is seldom available, especially for bacterial agents other than GBS. Further genomic studies may help investigate the role of vertical transmission in neonatal meningitis caused by other bacteria. Current indications for intrapartum antimicrobial drugs prophylaxis have been determined on the basis of risk factors for early onset GBS disease; therefore, intravenous penicillin G or ampicillin is often the standard empirical regimen used. However, if further research determines that the mother may also be a source of transmission for other bacterial agents, broader-spectrum antimicrobial drugs may need to be considered as treatment for intrapartum fever or prolonged rupture of membranes.

E. anophelis is likely an underreported bacterium because it can be easily misidentified as *E. meningoseptica*, which shares a similar phenotypic profile (*17,19*). The *E. anophelis* isolates from the recent outbreak reported in Singapore were initially mistakenly identified as *E. meningoseptica* (*19,36*). Of the 3 strains we identified, 2 were misidentified as *E. meningoseptica* with MALDI-TOF mass spectrometry, the state-of-the-art technology, which is replacing conventional phenotypic identification in diagnostic laboratories. The reason for failure of MALDI-TOF mass spectrometry to identify these strains was that reference *E. anophelis* strains are lacking in existing diagnostic spectrum databases, as is the case with other less commonly encountered organisms (*21*).

Although 16S rRNA gene sequencing should provide sufficient resolution, some strains indexed as *E. meningoseptica*, such as strains G3-1-08 and 502, were actually more closely related to *E. anophelis* than to *E. meningoseptica* in their 16S rRNA sequences (Figure 3; online Technical Appendix Figure 2) (*37*). These ambiguous, potentially misidentified strains may cause incorrect interpretations in suspected *E. anophelis* infections. For example, the sequence of strain HKU36 possessed 99.8% nucleotide identity to that of *E. meningingoseptica* strain G3-1-08 but only 99.1% nucleotide identity to that of *E. anophelis* strain R26^T. Furthermore, phenotypic tests such as acid production from cellobiose and citrate utilization, previously proposed to be useful for identification of *E. anophelis* (*15*), are probably unreliable in differentiating among *Elizabethkingia* species. For example, *E. anophelis* strain R26^T produces acid from cellobiose, but the 3 strains we identified do not; in addition, *E. anophelis* strains R26^T, HKU37, and HKU38, but not strain HKU36, utilize citrate (online Technical Appendix Table 1). Strain HKU36 displayed higher MIC of vancomycin than did strains HKU37 and HKU38 and type strains of *E. anophelis*, *E. meningoseptica*, and *E. miricola*, which correlates with previous reports on variable vancomycin susceptibilities in *Elizabethkingia* (*38,39*). The species identity of the 3 strains we identified was only resolved by intergenomic comparison. Inclusion of *E. anophelis* in MALDI-TOF MS databases and rectification of 16S rRNA gene sequences of *Elizabethkingia* strains deposited in databases will enable accurate diagnosis of more *E. anophelis* infections.

The draft genome sequences we identified have enabled rapid exploration of novel β-lactamase and other antimicrobial drug resistance genes and possible virulence genes in *E. anophelis*, highlighting the potential of genome sequencing in identifying novel drug-resistance mechanisms and guiding treatment regimens for emerging, multidrug-resistant bacteria (*25,34,40*). Because previous cases of *E. anophelis* neonatal meningitis have been associated with poor outcomes (*17,18*), further work to elucidate the pathogenesis and antimicrobial drug resistance patterns of this emerging pathogen may help improve clinical management of illness. The findings of potential genes related to neuroinvasion and acid tolerance and the unique genetic characteristics in clinical strains of *E. anophelis* compared with mosquito strains may also provide insights on the ability of *E. anophelis* to adapt to different ecologic niches and cause neonatal infection through vertical transmission.

In conclusion, the genome data we obtained for these cases offered superior discriminatory power that supported appropriate infection control measures. The ability to distinguish different bacterial isolates often has critical implications on practical infection-control management, but different strains of the same bacterial species may not be distinguishable by their phenotypes because they reflect a tiny portion of the microbial genome. With better automation and lower costs, draft genome sequencing, which

offers a short turnaround time, may replace existing typing methods such as PFGE or multilocus sequence typing for outbreak investigations.

Acknowledgments

We thank Cheung-Hing Foo for technical support in bacterial identification and members of the Centre for Genomic Sciences, The University of Hong Kong, for their technical support in genome sequencing.

This work was supported by Health and Medical Research Fund, Food and Health Bureau, The Government of the Hong Kong Special Administrative Region; Strategic Research Theme Fund, Committee for Research and Conference Grant, and University Development Fund, The University of Hong Kong; the Shaw Foundation; donation from Ms. Eunice Lam; and Consultancy Service for Enhancing Laboratory Surveillance of Emerging Infectious Disease for the HKSAR Department of Health.

Dr. Lau is a clinical professor in the Department of Microbiology at The University of Hong Kong. Her research focuses on microbial genomics for studying emerging infectious diseases.

References

1. Loman NJ, Constantinidou C, Chan JZ, Halachev M, Sergeant M, Penn CW, et al. High-throughput bacterial genome sequencing: an embarrassment of choice, a world of opportunity. Nat Rev Microbiol. 2012;10:599–606. http://dx.doi.org/10.1038/nrmicro2850
2. Fournier PE, Drancourt M, Raoult D. Bacterial genome sequencing and its use in infectious diseases. Lancet Infect Dis. 2007; 7:711–23. http://dx.doi.org/10.1016/S1473-3099(07)70260-8
3. Shah MA, Mutreja A, Thomson N, Baker S, Parkhill J, Dougan G, et al. Genomic epidemiology of *Vibrio cholerae* O1 associated with floods, Pakistan, 2010. Emerg Infect Dis. 2014;20:13–20. http://dx.doi.org/10.3201/.eid2001.130428
4. Snyder LA, Loman NJ, Faraj LA, Levi K, Weinstock G, Boswell TC, et al. Epidemiological investigation of *Pseudomonas aeruginosa* isolates from a six-year-long hospital outbreak using high-throughput whole genome sequencing. Euro Surveill. 2013;18:20611.
5. Harris SR, Cartwright EJ, Török ME, Holden MT, Brown NM, Ogilvy-Stuart AL, et al. Whole-genome sequencing for analysis of an outbreak of methicillin-resistant *Staphylococcus aureus*: a descriptive study. Lancet Infect Dis. 2013;13:130–6. http://dx.doi.org/10.1016/S1473-3099(12)70268-2
6. Walker TM, Ip CL, Harrell RH, Evans JT, Kapatai G, Dedicoat MJ, et al. Whole-genome sequencing to delineate *Mycobacterium tuberculosis* outbreaks: a retrospective observational study. Lancet Infect Dis. 2013;13:137–46. http://dx.doi.org/10.1016/S1473-3099(12)70277-3
7. Bryant JM, Grogono DM, Greaves D, Foweraker J, Roddick I, Inns T, et al. Whole-genome sequencing to identify transmission of *Mycobacterium abscessus* between patients with cystic fibrosis: a retrospective cohort study. Lancet. 2013;381:1551–60. http://dx.doi.org/10.1016/S0140-6736(13)60632-7
8. Tse H, Bao JY, Davies MR, Maamary P, Tsoi HW, Tong AH, et al. Molecular characterization of the 2011 Hong Kong scarlet fever outbreak. J Infect Dis. 2012;206:341–51. http://dx.doi.org/10.1093/infdis/jis362
9. Brown CC, Olsen RJ, Fittipaldi N, Morman ML, Fort PL, Neuwirth R, et al. Spread of virulent group A *Streptococcus* type emm59 from Montana to Wyoming, USA. Emerg Infect Dis. 2014;20:679–81. http://dx.doi.org/10.3201/eid2004.130564
10. Köser CU, Holden MT, Ellington MJ, Cartwright EJ, Brown NM, Ogilvy-Stuart AL, et al. Rapid whole-genome sequencing for investigation of a neonatal MRSA outbreak. N Engl J Med. 2012;366:2267–75. http://dx.doi.org/10.1056/NEJMoa1109910
11. Loman NJ, Constantinidou C, Christner M, Rohde H, Chan JZ, Quick J, et al. A culture-independent sequence-based metagenomics approach to the investigation of an outbreak of Shiga-toxigenic *Escherichia coli* O104:H4. JAMA. 2013;309:1502–10. http://dx.doi.org/10.1001/jama.2013.3231
12. Price JR, Golubchik T, Cole K, Wilson DJ, Crook DW, Thwaites GE, et al. Whole-genome sequencing shows that patient-to-patient transmission rarely accounts for acquisition of *Staphylococcus aureus* in an intensive care unit. Clin Infect Dis. 2014;58:609–18. http://dx.doi.org/10.1093/cid/cit807
13. Pérez-Lago L, Comas I, Navarro Y, González-Candelas F, Herranz M, Bouza E, et al. Whole genome sequencing analysis of intrapatient microevolution in *Mycobacterium tuberculosis*: potential impact on the inference of tuberculosis transmission. J Infect Dis. 2014;209:98–108. http://dx.doi.org/10.1093/infdis/jit439
14. Johnson PD, Ballard SA, Grabsch EA, Stinear TP, Seemann T, Young HL, et al. A sustained hospital outbreak of vancomycin-resistant *Enterococcus faecium* bacteremia due to emergence of vanB *E. faecium* sequence type 203. J Infect Dis. 2010;202: 1278–86. http://dx.doi.org/10.1086/656319
15. Kämpfer P, Matthews H, Glaeser SP, Martin K, Lodders N, Faye I. *Elizabethkingia anophelis* sp. nov., isolated from the midgut of the mosquito *Anopheles gambiae.* Int J Syst Evol Microbiol. 2011;61:2670–5. http://dx.doi.org/10.1099/ijs.0.026393-0
16. Kim KK, Kim MK, Lim JH, Park HY, Lee ST. Transfer of *Chryseobacterium meningosepticum* and *Chryseobacterium miricola* to *Elizabethkingia* gen. nov. as *Elizabethkingia meningoseptica* comb. nov. and *Elizabethkingia miricola* comb. nov. Int J Syst Evol Microbiol. 2005;55:1287–93. http://dx.doi.org/10.1099/ijs.0.63541-0
17. Frank T, Gody JC, Nguyen LB, Berthet N, Le Fleche-Mateos A, Bata P, et al. First case of *Elizabethkingia anophelis* meningitis in the Central African Republic. Lancet. 2013;381:1876. http://dx.doi.org/10.1016/S0140-6736(13)60318-9
18. Bobossi-Serengbe G, Gody JC, Beyam NE, Bercion R. First documented case of *Chryseobacterium meningosepticum* meningitis in Central African Republic. Med Trop (Mars). 2006;66:182–4.
19. Teo J, Tan SY, Tay M, Ding Y, Kjelleberg S, Givskov M, et al. First case of *E anophelis* outbreak in an intensive-care unit. Lancet. 2013;382:855–6. http://dx.doi.org/10.1016/S0140-6736(13)61858-9
20. Clinical and Laboratory Standards Institute. Performance standards for antimicrobial disk susceptibility tests. Approved standard, 11th ed. M02–A11. Wayne (PA): The Institute; 2012.
21. Lau SK, Tang BS, Curreem SO, Chan TM, Martelli P, Tse CW, et al. Matrix-assisted laser desorption ionization–time of flight mass spectrometry for rapid identification of *Burkholderia pseudomallei*: importance of expanding databases with pathogens endemic to different localities. J Clin Microbiol. 2012;50:3142–3. http://dx.doi.org/10.1128/JCM.01349-12
22. Woo PC, Lau SK, Teng JL, Que TL, Yung RW, Luk WK, et al. L Hongkongensis study group. Association of *Laribacter hongkongensis* in community-acquired gastroenteritis with travel and eating fish: a multicentre case-control study. Lancet. 2004;363:1941–7. http://dx.doi.org/10.1016/S0140-6736(04)16407-6
23. Lau SK, Curreem SO, Lin CC, Fung AM, Yuen KY, Woo PC. *Streptococcus hongkongensis* sp. nov., isolated from a patient with an infected puncture wound and from a marine flatfish.

Int J Syst Evol Microbiol. 2013;63:2570–6. http://dx.doi.org/10.1099/ijs.0.045120-0
24. Tse H, Tsoi HW, Leung SP, Lau SK, Woo PC, Yuen KY. Complete genome sequence of *Staphylococcus lugdunensis* strain HKU09–01. J Bacteriol. 2010;192:1471–2. http://dx.doi.org/10.1128/JB.01627-09
25. Woo PC, Lau SK, Tse H, Teng JL, Curreem SO, Tsang AK, et al. The complete genome and proteome of *Laribacter hongkongensis* reveal potential mechanisms for adaptations to different temperatures and habitats. PLoS Genet. 2009;5:e1000416. http://dx.doi.org/10.1371/journal.pgen.1000416
26. Delcher AL, Bratke KA, Powers EC, Salzberg SL. Identifying bacterial genes and endosymbiont DNA with Glimmer. Bioinformatics. 2007;23:673–9. http://dx.doi.org/10.1093/bioinformatics/btm009
27. Aziz RK, Bartels D, Best AA, DeJongh M, Disz T, Edwards RA, et al. The RAST server: rapid annotations using subsystems technology. BMC Genomics. 2008;9:75. http://dx.doi.org/10.1186/1471-2164-9-75
28. Liu B, Pop M. ARDB—antibiotic resistance genes database. Nucleic Acids Res. 2009;37:D443–7.http://dx.doi.org/10.1093/nar/gkn656
29. Auch AF, Klenk HP, Göker M. Standard operating procedure for calculating genome-to-genome distances based on high-scoring segment pairs. Stand Genomic Sci. 2010;2:142–8. http://dx.doi.org/10.4056/sigs.541628
30. Dussurget O. New insights into determinants of *Listeria monocytogenes* virulence. Int Rev Cell Mol Biol. 2008;270:1–38. http://dx.doi.org/10.1016/S1937-6448(08)01401-9
31. Kreft J, Vázquez-Boland JA, Altrock S, Dominguez-Bernal G, Goebel W. Pathogenicity islands and other virulence elements in *Listeria.* Curr Top Microbiol Immunol. 2002;264:109–25.
32. Hoffman JA, Badger JL, Zhang Y, Huang SH, Kim KS. *Escherichia coli* K1 *aslA* contributes to invasion of brain microvascular endothelial cells in vitro and in vivo. Infect Immun. 2000;68:5062–7. http://dx.doi.org/10.1128/IAI.68.9.5062-5067.2000
33. Cheng C, Chen J, Fang C, Xia Y, Shan Y, Liu Y, et al. *Listeria monocytogenes aguA1*, but not *aguA2*, encodes a functional agmatine deiminase: biochemical characterization of its catalytic properties and roles in acid tolerance. J Biol Chem. 2013;288:26606–15. http://dx.doi.org/10.1074/jbc.M113.477380
34. Matyi SA, Hoyt PR, Hosoyama A, Yamazoe A, Fujita N, Gustafson JE. Draft genome sequences of *Elizabethkingia meningoseptica.* Genome Announc. 2013;1:e00444–13. http://dx.doi.org/10.1128/genomeA.00444-13
35. Kukutla P, Lindberg BG, Pei D, Rayl M, Yu W, Steritz M, et al. Draft genome sequences of *Elizabethkingia anophelis* strains R26^T and Ag1 from the midgut of the malaria mosquito *Anopheles gambiae.* Genome Announc. 2013;1:e01030–13. http://dx.doi.org/10.1128/genomeA.01030-13
36. Balm MN, Salmon S, Jureen R, Teo C, Mahdi R, Seetoh T, et al. Bad design, bad practices, bad bugs: frustrations in controlling an outbreak of *Elizabethkingia meningoseptica* in intensive care units. J Hosp Infect. 2013;85:134–40. http://dx.doi.org/10.1016/j.jhin.2013.05.012
37. Quick J, Constantinidou C, Pallen MJ, Oppenheim B, Loman NJ. Draft genome sequence of *Elizabethkingia meningoseptica* isolated from a traumatic wound. Genome Announc. 2014;2:e00355–14. http://dx.doi.org/10.1128/genomeA.00355-14
38. Sarma S, Kumar N, Jha A, Baveja U, Sharma S. *Elizabethkingia meningosepticum*: an emerging cause of septicemia in critically ill patients. J Lab Physicians. 2011;3:62–3. http://dx.doi.org/10.4103/0974-2727.78575
39. Teo J, Tan SY, Liu Y, Tay M, Ding Y, Li Y, et al. Comparative genomic analysis of malaria mosquito vector-associated novel pathogen *Elizabethkingia anophelis.* Genome Biol Evol. 2014;6:1158–65. http://dx.doi.org/10.1093/gbe/evu094
40. Holden MT, Feil EJ, Lindsay JA, Peacock SJ, Day NP, Enright MC, et al. Complete genomes of two clinical *Staphylococcus aureus* strains: evidence for the rapid evolution of virulence and drug resistance. Proc Natl Acad Sci U S A. 2004;101:9786–91. http://dx.doi.org/10.1073/pnas.0402521101

Address for correspondence: Patrick C.Y. Woo, Department of Microbiology, The University of Hong Kong, Room 423, University Pathology Building, Queen Mary Hospital Compound, Pokfulam Road, Hong Kong, China; email: pcywoo@hkucc.hku.hk

Get the content you want delivered to your inbox.

Table of Contents
Podcasts
Ahead of Print Articles
CME
Specialized Content

Online subscription: wwwnc.cdc.gov/eid/subscribe.htm

Article DOI: http://dx.doi.org/10.3201/eid2102.140623

Evidence for *Elizabethkingia anophelis* Transmission from Mother to Infant, Hong Kong

Technical Appendix

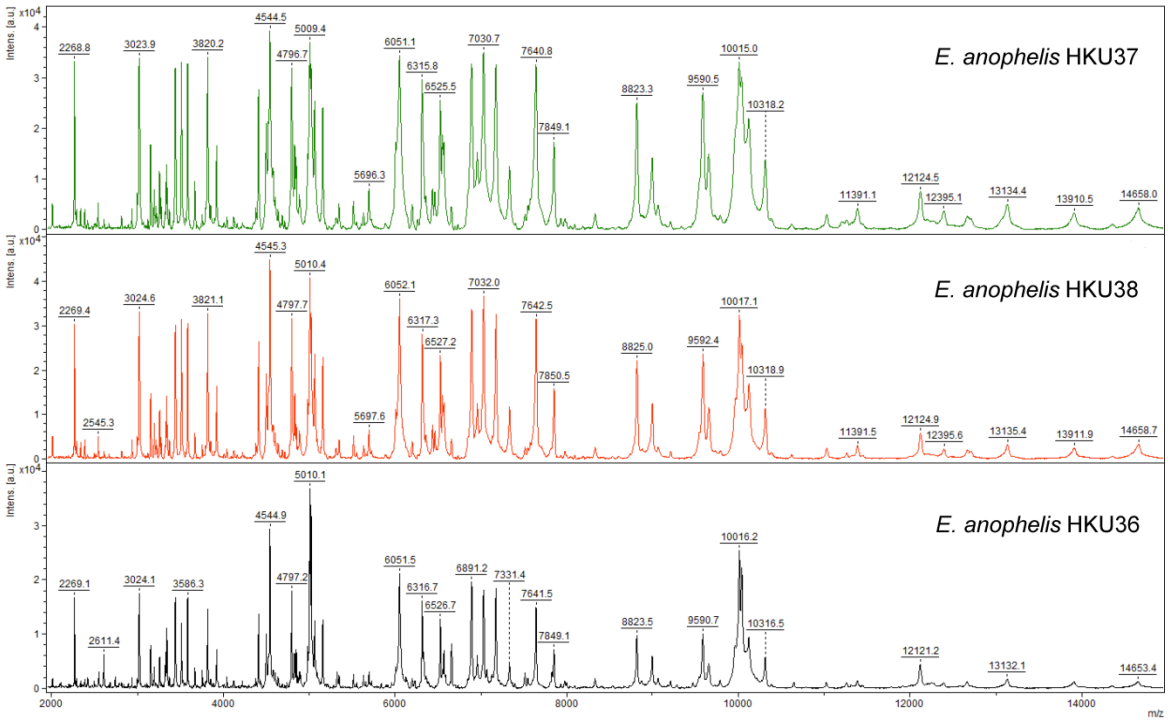

Technical Appendix Figure 1. Results of matrix-assisted laser desorption ionization/time-of-flight (MALDI-TOF) mass spectrometry identification of 3 *Elizabethkingia anophelis* strains from patients in Hong Kong (HKU36–38). In panel A, MALDI-TOF spectra of the three isolates are shown. In panel B, dendrogram was generated from hierarchical clustering of MALDI-TOF spectra of the three isolates and reference strains of *E. meningoseptica* and *E. miricola* available in database, using ClinProTools 3.0 (Bruker Daltonics, Bremen, Germany). Distances are displayed in relative units.

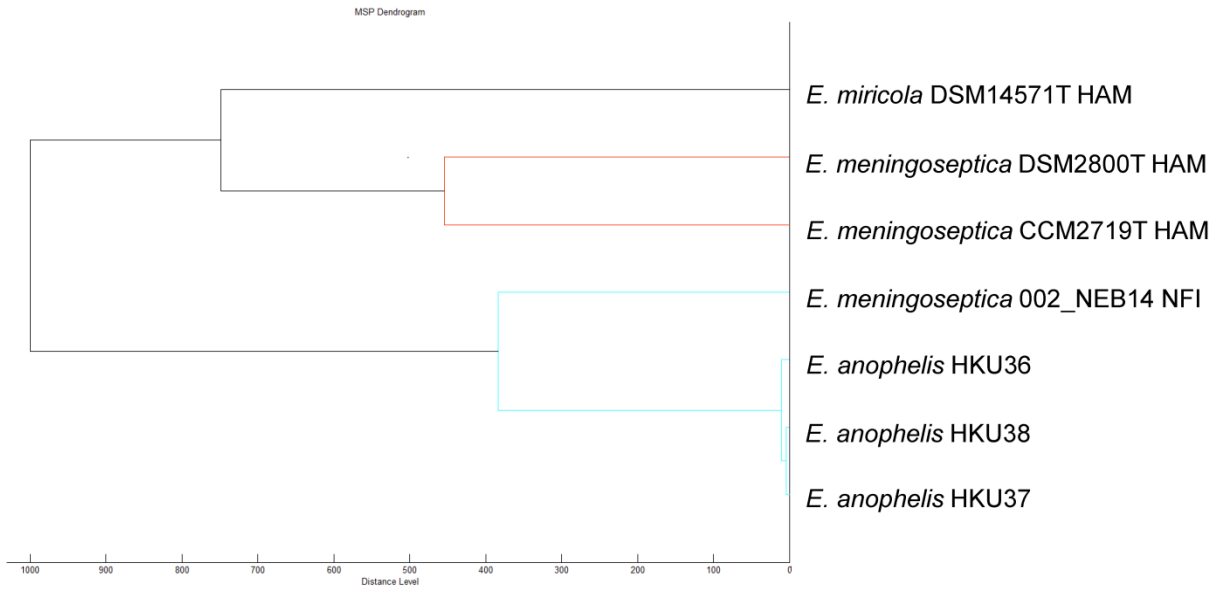

Technical Appendix Figure 2. Phylogenetic tree showing the relationship of the three *E. anophelis* strains HKU36-38 to closely related bacterial species using 16S rRNA gene sequence analysis. The tree was constructed by neighbour-joining method using *Chryseobacterium gleum* (AM232812.1) as the root. A total of 1317 nucleotide positions were included in the analysis. Bootstrap values were calculated from 1000 replicates. The scale bar indicates the estimated number of substitutions per 200 bases. Names and accession numbers are given as cited in GenBank database.

Technical Appendix Table 1. Phenotypic characteristics and vancomycin susceptibilities of the three *E. anophelis* clinical isolates compared to *E. anophelis* type strain R26^T, *E. meningoseptica* type strain ATCC 13253^T and *E. miricola* type strain LMG22470^T

Characteristics	*E. anophelis* strain HKU36	*E. anophelis* strain HKU37	*E. anophelis* strain HKU38	*E. anophelis* type strain R26^T	*E. meningoseptica* type strain ATCC 13253^T	*E. miricola* type strain LMG22470^T
Acid production from cellobiose	Negative	Negative	Negative	Positive	Negative	Weakly positive
Acid from melibiose	Negative	Negative	Negative	Negative	Positive	Weakly positive
Urea hydrolysis	Negative	Negative	Negative	Negative	Negative	Delayed positive
Citrate utilization	Negative	Delayed positive	Delayed positive	Delayed positive	Negative	Negative
Vancomycin MIC (µg/ml)	16	4	4	12	8	8

Technical Appendix Table 2. Results of draft genome assembly of the three *E. anophelis* isolates

Genome assembly data	Strain HKU36	Strain HKU37	Strain HKU38
Genome size	3.99 Mb	3.92 Mb	3.93 Mb
G + C content	35.4%	35.8%	35.8%
No. of contigs (>500 bp)	42	52	46
No. of predicted protein-coding genes	3667	3654	3662

Technical Appendix Table 3. Protein names and accession numbers of the 69 housekeeping genes used for phylogenetic analysis based on their concatenated sequences

No.	Gene	Description	*Elizabethkingia anophelis* Ag1	*Elizabethkingia anophelis* R26^T	*Elizabethkingia meningoseptica* ATCC 13253^T	'*Elizabethkingia meningoseptica*' 502	*Chryseobacterium gleum* ATCC 35910
1	*adk*	adenylate kinase	EHM99033.1	ELR78181.1	EOR29026.1	EQB93674.1	EFK36011.1
2	*aroC*	chorismate synthase protein	EHM98932.1	ELR79157.1	EOR30315.1	EQB91279.1	EFK36463.1
3	*aroE*	shikimate 5-dehydrogenase	EHM97099.1	ELR79534.1	EOR29119.1	EQB92826.1	EFK37041.1
4	*atpG*	ATP synthase gamma subunit	EHM97869.1	ELR77763.1	EOR29854.1	EQB90742.1	EFK34458.1
5	*clpX*	ATP-dependent Clp protease, ATP-binding subunit ClpX	EHM97147.1	ELR80137.1	EOR29258.1	EQB92999.1	EFK38075.1
6	*ddl*	D-alanine--D-alanine ligase	EHM98607.1	ELR80901.1	EOR30203.1	EQB91483.1	EFK37089.1
7	*dnaG*	DNA primase	EHM96290.1	ELR80281.1	EOR29602.1	EQB93431.1	EFK35645.1
8	*dnaJ*	molecular chaperone DnaJ	EHM97005.1	ELR79584.1	EOR30530.1	EQB91744.1	EFK33359.1
9	*dnaN*	DNA polymerase III beta subunit protein DnaN	EHM99096.1	ELR78117.1	EOR30852.1	EQB93614.1	EFK33728.1
10	*efp*	translation elongation factor (P) Efp	EHM96207.1	ELR79458.1	EOR31162.1	EQB92149.1	EFK33096.1
11	*engA*	GTP-binding protein EngA	EHM97976.1	ELR77871.1	EOR30120.1	EQB90633.1	EFK32926.1
12	*frr*	ribosome recycling factor	EHM97858.1	ELR77751.1	EOR28456.1	EQB90754.1	EFK34962.1
13	*ftsZ*	cell division protein	EHM96855.1	ELR79837.1	EOR29056.1	EQB92556.1	EFK37400.1
14	*gltA*	citrate synthase	EHM98067.1	ELR78920.1	EOR31281.1	EQB91049.1	EFK38000.1
15	*glyA*	serine hydroxymethyltransferase GlyA	EHM98156.1	ELR80729.1	EOR28516.1	EQB91465.1	EFK33053.1
16	*gmk*	Guanylate kinase	EHM98926.1	ELR79163.1	EOR30303.1	EQB91303.1	EFK36478.1
17	*groEL*	molecular chaperone GroEL	EHM99261.1	ELR77949.1	EOR28992.1	EQB91175.1	EFK36363.1
18	*gyrB*	DNA gyrase, subunit B	EHM97538.1	ELR80389.1	EOR28497.1	EQB90771.1	EFK35453.1
19	*hemD*	uroporphyrinogen-III synthase	EHM98513.1	ELR80039.1	EOR30745.1	EQB92637.1	EFK37767.1
20	*infC*	translation initiation factor IF-3	EHM98658.1	ELR78736.1	EOR28593.1	EQB91887.1	EFK34832.1
21	*lepA*	GTP-binding protein LepA	EHM96750.1	ELR79731.1	EOR30078.1	EQB92448.1	EFK37466.1
22	*metG*	Methionyl-tRNA synthetase	EHM97741.1	ELR80931.1	EOR30645.1	EQB92897.1	EFK35396.1
23	*murI*	glutamate racemase	EHM98602.1	ELR80896.1	EOR30198.1	EQB91488.1	EFK37084.1
24	*mutS*	DNA mismatch repair protein	EHM98490.1	ELR80062.1	EOR30770.1	EQB92613.1	EFK37559.1
25	*ndh*	NADH dehydrogenase	EHM97992.1	ELR77888.1	EOR30137.1	EQB90616.1	EFK36447.1
26	*nusA*	transcription elongation factor NusA	EHM98422.1	ELR79019.1	EOR31379.1	EQB91154.1	EFK37875.1
27	*pbpA*	penicillin-binding protein 2b	EHM96729.1	ELR79709.1	EOR31600.1	EQB92422.1	EFK37686.1
28	*pfkB*	Ribokinase	EHM99170.1	ELR78044.1	EOR30918.1	EQB93544.1	EFK35803.1
29	*pgi*	glucose-6-phosphate isomerase	EHM98320.1	ELR79898.1	EOR31480.1	EQB92300.1	EFK37251.1
30	*pgk*	phosphoglycerate kinase	EHM96766.1	ELR79747.1	EOR31635.1	EQB92464.1	EFK37486.1
31	*ppa*	manganese-dependent inorganic pyrophosphatase	EHM99474.1	ELR78442.1	EOR31031.1	EQB94005.1	EFK35025.1
32	*purE*	phosphoribosylaminoimidazole carboxylase catalytic subunit PurE	EHM96991.1	ELR79598.1	EOR30543.1	EQB91730.1	EFK33446.1
33	*purK*	phosphoribosylaminoimidazole carboxylase ATPase subunit PurK	EHM96987.1	ELR79602.1	EOR30546.1	EQB91726.1	EFK33442.1
34	*pyrG*	CTP synthetase	EHM99276.1	ELR77936.1	EOR29004.1	EQB92753.1	EFK36380.1
35	*recA*	ATP/GTP binding motif	EHM99302.1	ELR77910.1	EOR28705.1	EQB92692.1	EFK36418.1
36	*recG*	ATP-dependent DNA helicase, RecG	EHM97941.1	ELR77835.1	EOR28850.1	EQB90669.1	EFK36929.1
37	*recN*	DNA replication protein RecF	EHM98297.1	ELR79922.1	EOR31506.1	EQB92325.1	EFK37286.1
38	*ribE*	riboflavin synthase	EHM98833.1	ELR79259.1	EOR30511.1	EQB91401.1	EFK36589.1
39	*rodA*	Rod shape-determining protein rodA	EHM96730.1	ELR79710.1	EOR31601.1	EQB92423.1	EFK37687.1
40	*rplA*	50S ribosomal protein L1	EHM98921.1	ELR79169.1	EOR30297.1	EQB91309.1	EFK36283.1
41	*rplB*	50S ribosomal protein L2	EHM98093.1	ELR78947.1	EOR31308.1	EQB91075.1	EFK37967.1
42	*rplC*	50S ribosomal protein L3	EHM98096.1	ELR78950.1	EOR31311.1	EQB91078.1	EFK37964.1
43	*rplD*	50S ribosomal protein L4	EHM98095.1	ELR78949.1	EOR31310.1	EQB91077.1	EFK37965.1
44	*rplE*	50S ribosomal protein L5	EHM98085.1	ELR78938.1	EOR31299.1	EQB91066.1	EFK37976.1
45	*rplF*	50S ribosomal protein L6	EHM98082.1	ELR78935.1	EOR31296.1	EQB91063.1	EFK37979.1
46	*rplK*	50S ribosomal protein L11	EHM98920.1	ELR79170.1	EOR30296.1	EQB91310.1	EFK36282.1

No.	Gene	Description	*Elizabethkingia anophelis* Ag1	*Elizabethkingia anophelis* R26^{T}	*Elizabethkingia meningoseptica* ATCC 13253^{T}	'*Elizabethkingia meningoseptica*' 502	*Chryseobacterium gleum* ATCC 35910
47	*rplL*	50S ribosomal protein L7	EHM98923.1	ELR79167.1	EOR30299.1	EQB91307.1	EFK36285.1
48	*rplM*	50S ribosomal protein L13	EHM98809.1	ELR79283.1	EOR28625.1	EQB91425.1	EFK36554.1
49	*rplP*	50S ribosomal protein L16	EHM98090.1	ELR78943.1	EOR31304.1	EQB91071.1	EFK37971.1
50	*rplS*	50S ribosomal protein L19	EHM98689.1	ELR78767.1	EOR29634.1	EQB91859.1	EFK35532.1
51	*rplT*	50S ribosomal protein L20	EHM98656.1	ELR78734.1	EOR28591.1	EQB91889.1	EFK34839.1
52	*rpmA*	50S ribosomal protein L27	EHM96827.1	ELR79807.1	EOR29988.1	EQB92525.1	EFK37322.1
53	*rpoA*	DNA-directed RNA polymerase subunit alpha	EHM98071.1	ELR78924.1	EOR31285.1	EQB91053.1	EFK37989.1
54	*rpoB*	DNA-directed RNA polymerase subunit beta	EHM96382.1	ELR80997.1	EOR29540.1	EQB93109.1	EFK36289.1
55	*rpsB*	30S ribosomal protein S2	EHM98811.1	ELR79281.1	EOR28623.1	EQB91423.1	EFK36556.1
56	*rpsC*	30S ribosomal protein S3	EHM98091.1	ELR78944.1	EOR31305.1	EQB91072.1	EFK37970.1
57	*rpsE*	30S ribosomal protein S5	EHM98080.1	ELR78933.1	EOR31294.1	EQB91061.1	EFK37981.1
58	*rpsI*	30S ribosomal protein S9	EHM98810.1	ELR79282.1	EOR28624.1	EQB91424.1	EFK36555.1
59	*rpsJ*	30S ribosomal protein S10	EHM98112.1	ELR78966.1	EOR31325.1	EQB91094.1	EFK37949.1
60	*rpsK*	30S ribosomal protein S11	EHM98073.1	ELR78926.1	EOR31287.1	EQB91055.1	EFK37987.1
61	*rpsM*	30S ribosomal protein S13	EHM98074.1	ELR78927.1	EOR31288.1	EQB91056.1	EFK37986.1
62	*rpsS*	30S ribosomal protein S19	EHM98092.1	ELR78946.1	EOR31307.1	EQB91074.1	EFK37968.1
63	*sucA*	2-oxoglutarate dehydrogenase decarboxylase component	EHM99425.1	ELR78493.1	EOR30239.1	EQB93956.1	EFK34424.1
64	*alaS*	Alanyl-RNA synthetase	EHM96283.1	ELR80290.1	EOR29610.1	EQB93424.1	EFK35625.1
65	*tktA*	transketolase	EHM96930.1	ELR79660.1	EOR30604.1	EQB91663.1	EFK36754.1
66	*tpiA*	triosephosphate isomerase	EHM96304.1	ELR80267.1	EOR29585.1	EQB93446.1	EFK35642.1
67	*trpC*	indole-3-glycerol-phosphate synthase	EHM99573.1	ELR78343.1	EOR30932.1	EQB94109.1	EFK35468.1
68	*tsf*	elongation factor Ts	EHM98813.1	ELR79279.1	EOR28621.1	EQB91421.1	EFK36564.1
69	*uvrA*	excinuclease ABC A subunit UvrA	EHM97607.1	ELR80434.1	EOR29973.1	EQB90839.1	EFK34489.1

No.	Gene	Description	*Flavobacterium branchiophilum* FL-15	*Flavobacterium columnare* ATCC 49512	*Flavobacterium frigoris* PS1	*Flavobacterium indicum* GPTSA100-9	*Flavobacterium johnsoniae* UW101	*Flavobacterium rivuli* DSM21788	*Flavobacterium psychrophilum* JIP02/86	*Weeksella virosa* DSM16922
1	*adk*	adenylate kinase	YP_004843328.1	YP_004942855.1	EIA10324.1	YP_005356587.1	YP_001192775.1	WP_020212144.1	YP_001296253.1	YP_004238641.1
2	*aroC*	chorismate synthase protein	YP_004843241.1	YP_004941761.1	EIA07987.1	YP_005357433.1	YP_001196894.1	WP_020215022.1	YP_001295684.1	YP_004239059.1
3	*aroE*	shikimate 5-dehydrogenase	YP_004844535.1	YP_004940842.1	EIA08302.1	YP_005357053.1	YP_001194935.1	WP_020211950.1	YP_001296643.1	YP_004237502.1
4	*atpG*	ATP synthase gamma subunit	YP_004842530.1	YP_004942235.1	EIA10015.1	YP_005358512.1	YP_001193412.1	WP_020214871.1	YP_001297311.1	YP_004238492.1
5	*clpX*	ATP-dependent Clp protease, ATP-binding subunit ClpX	YP_004843243.1	YP_004941516.1	EIA09493.1	YP_005356442.1	YP_001194054.1	WP_020213425.1	YP_001296948.1	YP_004238734.1
6	*ddl*	D-alanine--D-alanine ligase	YP_004844026.1	YP_004941995.1	EIA08323.1	YP_005357292.1	YP_001194964.1	WP_020211540.1	YP_001295574.1	YP_004237806.1
7	*dnaG*	DNA primase	YP_004844608.1	YP_004941419.1	EIA09098.1	YP_005358326.1	YP_001194141.1	WP_020213753.1	YP_001296936.1	YP_004239226.1
8	*dnaJ*	molecular chaperone DnaJ	YP_004844765.1	YP_004942990.1	EIA07801.1	YP_005356894.1	YP_001194720.1	WP_020211830.1	YP_001295590.1	YP_004239321.1
9	*dnaN*	DNA polymerase III beta subunit protein DnaN	YP_004843556.1	YP_004942175.1	EIA07252.1	YP_005357766.1	YP_001195061.1	WP_020211708.1	YP_001295990.1	YP_004237708.1
10	*efp*	translation elongation factor (P) Efp	YP_004844349.1	YP_004940702.1	EIA07534.1	YP_005357424.1	YP_001195241.1	WP_020211751.1	YP_001295882.1	YP_004237795.1
11	*engA*	GTP-binding protein EngA	YP_004844816.1	YP_004942744.1	EIA09193.1	YP_005358203.1	YP_001194230.1	WP_020213093.1	YP_001296829.1	YP_004238212.1
12	*frr*	ribosome recycling factor	YP_004845164.1	YP_004941270.1	EIA09266.1	YP_005358624.1	YP_001192929.1	WP_020213359.1	YP_001295365.1	YP_004239294.1
13	*ftsZ*	cell division protein	YP_004843062.1	YP_004941396.1	EIA09118.1	YP_005358278.1	YP_001194165.1	WP_020213744.1	YP_001296917.1	YP_004237973.1
14	*gltA*	citrate synthase	YP_004844776.1	YP_004941349.1	EIA10264.1	YP_005356640.1	YP_001192722.1	WP_020213492.1	YP_001296202.1	YP_004238792.1
15	*glyA*	serine hydroxymethyltransferase GlyA	YP_004844321.1	YP_004941760.1	EIA08001.1	YP_005357155.1	YP_001195743.1	WP_020211164.1	YP_001295601.1	YP_004238585.1
16	*gmk*	Guanylate kinase	YP_004845194.1	YP_004943171.1	EIA10106.1	YP_005357890.1	YP_001193096.1	WP_020212935.1	YP_001295279.1	YP_004237674.1
17	*groEL*	molecular chaperone GroEL	YP_004844224.1	YP_004942930.1	EIA09161.1	YP_005358225.1	YP_001194193.1	WP_020214765.1	YP_001296851.1	YP_004237859.1

No.	Gene	Description	*Flavobacterium branchiophilum* FL-15	*Flavobacterium columnare* ATCC 49512	*Flavobacterium frigoris* PS1	*Flavobacterium indicum* GPTSA100-9	*Flavobacterium johnsoniae* UW101	*Flavobacterium rivuli* DSM21788	*Flavobacterium psychrophilum* JIP02/86	*Weeksella virosa* DSM16922
18	*gyrB*	DNA gyrase, subunit B	YP_004843747.1	YP_004941981.1	EIA08992.1	YP_005357836.1	YP_001194601.1	WP_020212750.1	YP_001295451.1	YP_004238535.1
19	*hemD*	uroporphyrinogen-III synthase	YP_004843024.1	YP_004943282.1	EIA09279.1	YP_005358593.1	YP_001192910.1	WP_020213377.1	YP_001295118.1	YP_004238559.1
20	*infC*	translation initiation factor IF-3	YP_004844738.1	YP_004940781.1	EIA10498.1	YP_005356931.1	YP_001192382.1	WP_020215189.1	YP_001295810.1	YP_004238548.1
21	*lepA*	GTP-binding protein LepA	YP_004844927.1	YP_004942415.1	EIA10160.1	YP_005358664.1	YP_001193139.1	WP_020212956.1	YP_001297099.1	YP_004238325.1
22	*metG*	Methionyl-tRNA synthetase	YP_004845262.1	YP_004942277.1	EIA09859.1	YP_005358540.1	YP_001193210.1	WP_020214992.1	YP_001294995.1	YP_004238214.1
23	*murI*	glutamate racemase	YP_004844480.1	YP_004941529.1	EIA09443.1	YP_005356427.1	YP_001194038.1	WP_020213207.1	YP_001296963.1	YP_004239318.1
24	*mutS*	DNA mismatch repair protein	YP_004842808.1	YP_004941508.1	EIA09506.1	YP_005358374.1	YP_001194074.1	WP_020212380.1	YP_001295324.1	YP_004238747.1
25	*ndh*	NADH dehydrogenase	YP_004844830.1	YP_004941835.1	EIA07632.1	YP_005356809.1	YP_001195192.1	WP_020211712.1	YP_001296799.1	YP_004239336.1
26	*nusA*	transcription elongation factor NusA	YP_004842699.1	YP_004942659.1	EIA09378.1	YP_005356369.1	YP_001193980.1	WP_020213406.1	YP_001295398.1	YP_004238583.1
27	*pbpA*	penicillin-binding protein 2b	YP_004842581.1	YP_004941462.1	EIA09649.1	YP_005356495.1	YP_001193806.1	WP_020212211.1	YP_001297275.1	YP_004238739.1
28	*pfkB*	Ribokinase	YP_004845172.1	YP_004943205.1	EIA10148.1	YP_005358652.1	YP_001193483.1	WP_020213838.1	YP_001295133.1	YP_004238344.1
29	*pgi*	glucose-6-phosphate isomerase	YP_004842585.1	YP_004942598.1	EIA10132.1	YP_005358681.1	YP_001193089.1	WP_020213880.1	YP_001295083.1	YP_004238140.1
30	*pgk*	phosphoglycerate kinase	YP_004842563.1	YP_006194203.1	EIA09930.1	YP_005356095.1	YP_001193329.1	WP_020214854.1	YP_001294958.1	YP_004238305.1
31	*ppa*	manganese-dependent inorganic pyrophosphatase	YP_004842932.1	YP_004941449.1	EIA09673.1	YP_005356512.1	YP_001193829.1	WP_020212182.1	YP_001295270.1	YP_004238254.1
32	*purE*	phosphoribosylaminoimidazole carboxylase catalytic subunit PurE	YP_004844610.1	YP_004942860.1	EIA10328.1	YP_005356582.1	YP_001192781.1	WP_020213481.1	YP_001296257.1	YP_004238035.1
33	*purK*	phosphoribosylaminoimidazole carboxylase ATPase subunit PurK	YP_004844366.1	YP_004942857.1	EIA10327.1	YP_005356584.1	YP_001192780.1	WP_020213480.1	YP_001296256.1	YP_004238034.1
34	*pyrG*	CTP synthetase	YP_004843652.1	YP_004941223.1	EIA09061.1	YP_005357320.1	YP_001194729.1	WP_020212691.1	YP_001296767.1	YP_004237877.1
35	*recA*	ATP/GTP binding motif	YP_004844934.1	YP_004942626.1	EIA09935.1	YP_005358697.1	YP_001193340.1	WP_020212902.1	YP_001297102.1	YP_004238617.1
36	*recG*	ATP-dependent DNA helicase, RecG	YP_004844110.1	YP_004941087.1	EIA07485.1	YP_005357092.1	YP_001195275.1	WP_020211315.1	YP_001295915.1	YP_004239004.1
37	*recN*	DNA replication protein RecF	YP_004844143.1	YP_004942028.1	EIA08410.1	YP_005357867.1	YP_001195798.1	WP_020211306.1	YP_001296710.1	YP_004239260.1
38	*ribE*	riboflavin synthase	YP_004842654.1	YP_004942234.1	EIA09229.1	YP_005358530.1	YP_001193004.1	WP_020215095.1	YP_001297239.1	YP_004238363.1
39	*rodA*	Rod shape-determining protein rodA	YP_004842582.1	YP_004941463.1	EIA09648.1	YP_005356494.1	YP_001193805.1	WP_020212212.1	YP_001297276.1	YP_004238738.1
40	*rplA*	50S ribosomal protein L1	YP_004843132.1	YP_004942684.1	EIA08871.1	YP_005358134.1	YP_001194291.1	WP_020211976.1	YP_001296077.1	YP_004238016.1
41	*rplB*	50S ribosomal protein L2	YP_004844803.1	YP_004942809.1	EIA10291.1	YP_005356613.1	YP_001192749.1	WP_020213637.1	YP_001296230.1	YP_004238655.1
42	*rplC*	50S ribosomal protein L3	YP_004844806.1	YP_004942812.1	EIA10294.1	YP_005356610.1	YP_001192752.1	WP_020213634.1	YP_001296233.1	YP_004238652.1
43	*rplD*	50S ribosomal protein L4	YP_004844805.1	YP_004942811.1	EIA10293.1	YP_005356611.1	YP_001192751.1	WP_020213635.1	YP_001296232.1	YP_004238653.1
44	*rplE*	50S ribosomal protein L5	YP_004844794.1	YP_004942800.1	EIA10282.1	YP_005356622.1	YP_001192740.1	WP_020213645.1	YP_001296221.1	YP_004238664.1
45	*rplF*	50S ribosomal protein L6	YP_004844791.1	YP_004942797.1	EIA10279.1	YP_005356625.1	YP_001192737.1	WP_020213648.1	YP_001296218.1	YP_004238672.1
46	*rplK*	50S ribosomal protein L11	YP_004843131.1	YP_004942685.1	EIA08870.1	YP_005358135.1	YP_001194290.1	WP_020211977.1	YP_001296078.1	YP_004238017.1
47	*rplL*	50S ribosomal protein L7	YP_004843134.1	YP_004942682.1	EIA08873.1	YP_005358132.1	YP_001194293.1	WP_020211974.1	YP_001296075.1	YP_004238014.1
48	*rplM*	50S ribosomal protein L13	YP_004842586.1	YP_004941282.1	EIA09368.1	YP_005356488.1	YP_001193963.1	WP_020214767.1	YP_001295385.1	YP_004238816.1
49	*rplP*	50S ribosomal protein L16	YP_004844799.1	YP_004942805.1	EIA10287.1	YP_005356617.1	YP_001192745.1	WP_020213641.1	YP_001296226.1	YP_004238659.1
50	*rplS*	50S ribosomal protein L19	YP_004845156.1	YP_004943082.1	EIA08132.1	YP_005356916.1	YP_001194529.1	WP_020212560.1	YP_001296742.1	YP_004237673.1
51	*rplT*	50S ribosomal protein L20	YP_004844740.1	YP_004940779.1	EIA10500.1	YP_005356929.1	YP_001192384.1	WP_020215187.1	YP_001295808.1	YP_004238550.1
52	*rpmA*	50S ribosomal protein L27	YP_004842988.1	YP_004940654.1	EIA09345.1	YP_005356480.1	YP_001193897.1	WP_020212342.1	YP_001297073.1	YP_004238403.1
53	*rpoA*	DNA-directed RNA polymerase subunit alpha	YP_004844780.1	YP_004942786.1	EIA10269.1	YP_005356636.1	YP_001192726.1	WP_020213657.1	YP_001296207.1	YP_004238683.1
54	*rpoB*	DNA-directed RNA polymerase subunit beta	YP_004843135.1	YP_004942681.1	EIA08874.1	YP_005358131.1	YP_001194294.1	WP_020211973.1	YP_001296074.1	YP_004238013.1
55	*rpsB*	30S ribosomal protein S2	YP_004842588.1	YP_004941280.1	EIA09366.1	YP_005356486.1	YP_001193961.1	WP_020214769.1	YP_001295383.1	YP_004238818.1
56	*rpsC*	30S ribosomal protein S3	YP_004844800.1	YP_004942806.1	EIA10288.1	YP_005356616.1	YP_001192746.1	WP_020213640.1	YP_001296227.1	YP_004238658.1
57	*rpsE*	30S ribosomal protein S5	YP_004844789.1	YP_004942795.1	EIA10277.1	YP_005356627.1	YP_001192735.1	WP_020213650.1	YP_001296216.1	YP_004238674.1
58	*rpsI*	30S ribosomal protein S9	YP_004842587.1	YP_004941281.1	EIA09367.1	YP_005356487.1	YP_001193962.1	WP_020214768.1	YP_001295384.1	YP_004238817.1
59	*rpsJ*	30S ribosomal protein S10	YP_004844837.1	YP_004942813.1	EIA10295.1	YP_005356609.1	YP_001192753.1	WP_020213633.1	YP_001296234.1	YP_004238651.1
60	*rpsK*	30S ribosomal protein S11	YP_004844782.1	YP_004942788.1	EIA10271.1	YP_005356634.1	YP_001192728.1	WP_020213655.1	YP_001296209.1	YP_004238681.1
61	*rpsM*	30S ribosomal protein S13	YP_004844783.1	YP_004942789.1	EIA10272.1	YP_005356633.1	YP_001192729.1	WP_020213654.1	YP_001296210.1	YP_004238680.1

No.	Gene	Description	*Flavobacterium branchiophilum* FL-15	*Flavobacterium columnare* ATCC 49512	*Flavobacterium frigoris* PS1	*Flavobacterium indicum* GPTSA100-9	*Flavobacterium johnsoniae* UW101	*Flavobacterium rivuli* DSM21788	*Flavobacterium psychrophilum* JIP02/86	*Weeksella virosa* DSM16922
62	*rpsS*	30S ribosomal protein S19	YP_004844802.1	YP_004942808.1	EIA10290.1	YP_005356614.1	YP_001192748.1	WP_020213638.1	YP_001296229.1	YP_004238656.1
63	*sucA*	2-oxoglutarate dehydrogenase decarboxylase component	YP_004842676.1	YP_004942519.1	EIA09805.1	YP_005356282.1	YP_001193607.1	WP_020212406.1	YP_001297263.1	YP_004237778.1
64	*alaS*	Alanyl-RNA synthetase	YP_004844354.1	YP_004942759.1	EIA09202.1	YP_005358194.1	YP_001194245.1	WP_020213083.1	YP_001296809.1	YP_004238610.1
65	*tktA*	transketolase	YP_004844684.1	YP_004940771.1	EIA10540.1	YP_005357074.1	YP_001192406.1	WP_020211810.1	YP_001295603.1	YP_004237843.1
66	*tpiA*	triosephosphate isomerase	YP_004843541.1	YP_004942119.1	EIA08379.1	YP_005356847.1	YP_001195837.1	WP_020212471.1	YP_001296314.1	YP_004238777.1
67	*trpC*	indole-3-glycerol-phosphate synthase	YP_004844164.1	YP_004940849.1	EIA08447.1	YP_005357469.1	YP_001197212.1	WP_020212759.1	YP_001295434.1	YP_004238220.1
68	*tsf*	elongation factor Ts	YP_004842589.1	YP_004941279.1	EIA09365.1	YP_005356485.1	YP_001193960.1	WP_020214770.1	YP_001295382.1	YP_004238819.1
69	*uvrA*	excinuclease ABC A subunit UvrA	YP_004843715.1	YP_004940827.1	EIA07181.1	YP_005357832.1	YP_001196827.1	WP_020211841.1	YP_001295765.1	YP_004237701.1